Meteoritics 25, 101–113 (1990)

Deformation and thermal histories of chondrules in the Chainpur (LL3.4) chondrite

ALEX RUZICKA
Department of Planetary Sciences, University of Arizona, Tucson, AZ 85721 USA

(*Received 20 October 1989; accepted in revised form 26 January 1990*)

Abstract—Transmission-electron-microscopy (TEM) and optical data suggest that chondrules in the Chainpur (LL3.4) chondrite experienced varied thermal and deformation histories prior to the final agglomeration of the meteorite. Chainpur may be regarded as an agglomerate or breccia that experienced little deformation or heating during and after the final accumulation and compaction of its constituents.

One chondrule in Chainpur was impact-shocked to high pressures (~20–50 GPa), almost certainly prior to final agglomeration, either while it was an independent entity in space or while it was in the regolith of a parent body. However, most (>85%) of the chondrules in Chainpur were evidently not significantly shock-metamorphosed subsequent to their formation. The dearth of shock effects implies that most chondrules in Chainpur did not form by shock melting, although some chondrules may have formed by this process.

Dusty-metal-bearing olivine grains, which are widely interpreted to have escaped melting during chondrule formation, contain moderate densities of dislocations (~10^8 cm^{-2}). The dislocations in these grains were introduced before or during the last episode of melting in at least one chondrule. This observation can be explained if olivine was impact-deformed before or during chondrule formation, or if olivine was strained by reduction or thermally-induced processes during chondrule formation.

Low-Ca pyroxene grains in chondrules are often strained. In most cases this strain probably arose as a by-product of polytype transformations (protoenstatite → clinoenstatite/orthoenstatite and clinoenstatite → orthoenstatite) that occurred during the igneous crystallization and static annealing of chondrules.

Droplet chondrules with glassy mesostases were minimally annealed, consistent with an origin as relatively rapidly cooled objects in an unconfined, cold environment. Some irregular chondrules and at least one droplet chondrule were thermally metamorphosed prior to final agglomeration, either as a result of moderately slow cooling (~100 °C/hr) from melt temperatures (during autometamorphism) or as a result of reheating episodes. Two of the most annealed chondrules contain relatively abundant plagioclase feldspar, and one of these has a uniform olivine composition appropriate to that of an LL4 chondrite.

INTRODUCTION

TRANSMISSION-ELECTRON-MICROSCOPY (TEM) has proven invaluable for unraveling the histories of many chondritic meteorites, particularly with regard to such processes as metamorphism, shock deformation, aqueous alteration, and impact-induced lithification (*e.g.,* Ashworth and Barber, 1976, 1977; Barber, 1981). Although different meteorites were clearly affected by secondary (thermal metamorphism) and tertiary (shock) processes to different degrees, comparatively little TEM work has been done on examining a single chondrite for intrachondrite variations in deformation or thermal history. Such variations, if they exist, could be important for understanding the processes that affected chondrites prior to the final compaction and lithification (agglomeration) of their constituents.

In this paper, the results of optical and TEM studies of chondrules in the Chainpur (LL3.4) chondrite are presented. Type 3 chondrites, of which Chainpur is an example, show textural and mineralogical evidence of having experienced less aqueous alteration and less thermal metamorphism than chondrites belonging to Types 1–2 and 4–7, respectively (*e.g.,* McSween *et al.,* 1988). That Chainpur experienced little late, bulk heating is suggested by its low thermoluminescence sensitivity (appropriate to subtype 3.4—Sears *et al.,* 1980), and its generally high U,Th-He and K-Ar gas retention ages (>3.8 Ga) (Heymann and Mazor, 1968).

This study is patterned after that of Dodd (1971, 1974), who systematically examined chondrules in the Sharps (H3.4) and Hallingeberg (L3) meteorites using optical and microprobe techniques. Dodd (1971, 1974) concluded that virtually all of the chondrules in those two meteorites showed evidence for shock metamorphism and that this process played an important role in the genesis of chondrules. In addition, noting that chondrules in some Type 3 chondrites showed various degrees of chemical equilibration, Dodd (1971, 1974) and Scott (1984) suggested that chondrules were often thermally metamorphosed before the final agglomeration of the host meteorites.

In this study, optical petrography and microprobe work were followed by electron microscopy of selected chondrules. These objects include classic droplet chondrules (objects with smooth, circular or oval outlines), a droplet fragment (obviously a broken droplet chondrule), and irregular chondrules (objects that lack smooth, circular or oval outlines). Irregular chondrules have been termed clast chondrules by Dodd (1981, pp. 30–34), who also provided illustrations of these objects. A point of potential confusion is that the droplet fragment chondrules and irregular chondrules of this study appear to correspond to Wlotzka's (1983) "irregular chondrules" and "chondrule fragments," respectively. Previous TEM studies showed that while some droplet chondrules from Parnallee (LL3.6), Tieschitz (H3.6) and Chainpur are largely undeformed (Ashworth and Barber, 1977; Ashworth, 1981; Töpel-Schadt and Müller, 1985), at least one olivine-rich "rock fragment" (apparently an irregular chondrule) in Parnallee is heavily shocked (Ashworth and Barber, 1977; Ashworth, 1981).

EXPERIMENTAL

Approximately 1 g of Chainpur, consisting of more than a dozen separate pieces, was used to prepare twelve 30–40 μm-thick thin-sections for optical petrography and microprobe studies. Three thin sections of Carraweena (L3) were also prepared. Quantitative (wavelength-dispersive) microchemical analyses for Mg, Fe, Si, and Ca were obtained for chondrule olivine and pyroxene using an ARL EMX-SM electron microprobe at the Department of Earth and Space Sciences at S.U.N.Y., Stony Brook, following the procedure given by Ruzicka (1988). The

TABLE 1. Optical criteria for assigning deformation levels to olivine and pyroxene.

Deformation level	Criteria	Possible shock facies[1]
0	uniform extinction	a
1	possible slight undulose extinction	a?
2	mainly undulose extinction	b–c
3	undulose-mosaic extinction	b–d
4	mosaic extinction + intense fracturing (microbrecciation)	e
5	plastic deformation + recovery or recrystallization	e–f
6	extensive recovery or recrystallization (crystalloblastic texture)	f

[1] Dodd and Jarosewich (1979).

precision of the analyses is estimated to be ~0.3 wt.% for SiO_2, ~0.1 wt.% for FeO, ~0.2 wt.% for MgO and ~0.02 wt.% for CaO, based on repeat analyses of the unknowns.

Subsequent to microprobe work the samples were demounted from their slides by immersing them in acetone overnight, which dissolved the Crystalbond adhesive. Selected chondrules were gently disaggregated from the demounted thin-sections with a scalpel, and each separated chondrule (along with any adhering matrix) was mounted on a Cu grid with epoxy adhesive. The chondrules were then ion-milled until targeted areas became electron-transparent (<1 μm thick). Typically, each chondrule was ion-milled in 2–3 stages and TEM observations were performed after each stage of ion-milling, which maximized the total area that could be observed in each chondrule with TEM. Electron microscopy was performed using a JEM 200CX scanning-transmission-electron-microscope (STEM) at the Department of Earth and Space Sciences, S.U.N.Y. at Stony Brook. The STEM was operated at an accelerating voltage of 200 keV at a typical magnification of 50 000–100,000×. All imaging was done in bright field mode. Analytical-electron-microscopy (AEM) and selected-area-electron-diffraction (SAED) were used to aid in phase identification, and AEM data allowed qualitative analyses of phase compositions to be obtained.

OBSERVATIONS

One-hundred-eighteen objects (114 chondrules, and 4 large, isolated grains of olivine) in Chainpur were examined optically for evidence of deformation. Olivine and pyroxene were assigned deformation levels ranging from 0 to 6, using criteria (Table 1) consistent with the known response of olivine and low-Ca pyroxene to shock (*e.g.,* Stöffler *et al.,* 1988). Deformation levels were assigned independently to olivine and pyroxene, although the initial assumption was that the response of the two minerals to shock would be similar.

Fourteen of the chondrules were observed with a scanning-transmission-electron-microscope (STEM). Petrographic and microchemical data for these chondrules are summarized in Table 2, and their olivine compositions (where available) are shown in Fig. 1.

In this paper, chondrules are designated by letter prefixes which represent thin sections, and by number suffixes which represent different objects from each section. Most of the chondrules examined with TEM were selected as part of a systematic electron microscope investigation of adjacent chondrules in three small sections (C, D, G); 7 chondrules in close proximity to one another were observed with TEM in section C (Fig. 2).

In addition, three chondrules (KA1, KA10, MA2) of special interest from two other sections were also examined with TEM. KA1 is notable for the relatively uniform composition of its olivine (Fa_{29}), appropriate to that of an LL4 chondrite (Fig. 1), while MA2 contains an unusually coarse grain or cluster of grains (~650 μm across) of dusty-metal-bearing olivine. Dusty-metal-bearing olivine grains are of particular interest because these grains are generally considered to have escaped melting during chondrule formation; such grains represent either unmelted relicts of chondrule precursors, or xenocrysts that were incorporated into molten chondrules (Nagahara, 1981; Rambaldi, 1981; Kracher *et al.,* 1984). Some euhedral olivine pheno-

TABLE 2. Chainpur chondrules observed with TEM.

Object	Apparent diameter (μm)[1]	Textural type[2]	Form[3]	Olivine (Fa%)[4]	Low-Ca pyroxene (Fs%)[4]	Deformation level[5]
C1	1400	PO	droplet	0–5	–	ol 1, dol 0
C2	2150	PPO	irregular	14–19	12–15	tpx 1, upx 3, ol 2
C3	1310	EXP	droplet	13–24	<10	upx 2, ol 0
C4	720	POP	droplet	na	<10	ol 1, upx 2
C5	610	PP	droplet frag	–	<10	upx 2, tpx 0, ol 1
C6	950	PO	irregular	18–33	20–26	tpx 0, upx 3, ol 1
C8	450	PO	irregular	19–22	14–17	ol 0?, upx 2
D2	410	PO	droplet	1–4	–	ol 1
G1	750	PO	droplet	3–4	–	ol 0
G5	190	o	irregular	9–14	–	ol 3
G6	220	p	irregular	–	8–11	upx 4
KA1	1340	PO	irregular	29	–	ol 1
KA10	810	PO	irregular	24–34	–	ol 1
MA2	940	o	irregular	3–11	1–4	dol 0, ol 1

[1] Approximate maximum diameters. Value for C3 includes rim.
[2] PO = microporphyritic olivine; PP = microporphyritic pyroxene; POP = microporphyritic olivine-pyroxene; PPO = microporphyritic pyroxene, with pyroxene poikilitically enclosing olivine; EXP = excentroradial pyroxene; o = olivine-rich object; p = pyroxene-rich object.
[3] Form: droplet = object bounded by smooth circular or oval outline; droplet fragment = object partly bounded by smooth circular outline; irregular = object lacks smooth circular or oval outline.
[4] Typical composition of grains in mol% fayalite (Fa) and ferrosilite (Fs), generally based on 10–60 microprobe analyses per phase per chondrule (except C3, C4 and C5 pyroxene values, based on AEM data). Data for C3 olivine refers to coarse grains in dark rim. na = not analyzed.
[5] Criteria given in Table 1. ol = olivine; upx = optically untwinned low-Ca pyroxene; tpx = optically twinned low-Ca pyroxene; dol = dusty-metal-bearing olivine.

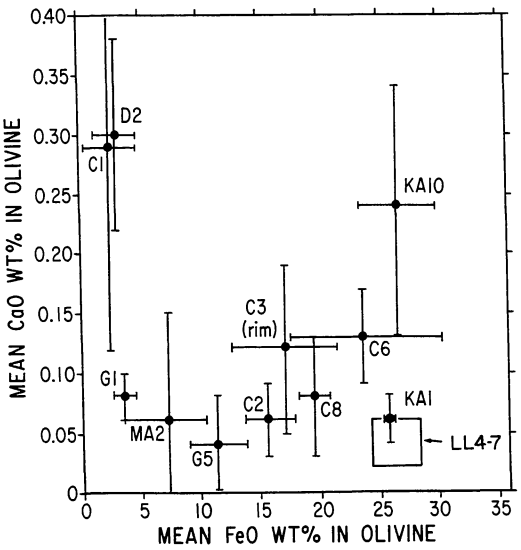

FIG. 1. Mean composition and compositional heterogeneity (±1 standard deviation of the mean) of olivine in Chainpur chondrules investigated with TEM, based on microprobe data (10–168 analyses per chondrule). The boxed area represents the range of mean compositions for olivine in LL4-7 chondrites (Heyse, 1979). Among ~60 Chainpur chondrules studied in detail with a microprobe, KA1 has the most uniform olivine composition and is the only chondrule whose olivine composition overlaps the LL4-7 field.

crysts in KA10 show what appear to be optically visible subgrains (Fig. 3), a texture that was also observed in 7 other Chainpur chondrules not examined with TEM.

Optical Evidence for Deformation

Approximately 85% of the 90 olivine-bearing chondrules examined optically show either uniform or barely perceptible undulose extinction in olivine (Fig. 4). This implies that most of the chondrules in Chainpur are unshocked, or that they were shocked to pressures <5–7 GPa, the minimum shock pressure known to produce undulose extinction in olivine (Sears *et al.*, 1984; Stöffler *et al.*, 1988). In many cases, it is possible that apparent slight undulose extinction in small olivine grains is an artifact caused by chondrule groundmass overlapping onto the olivine. Dusty-metal-bearing olivine grains also appear to show uniform or weak undulose extinction (Fig. 4). Roughly 15% of the olivine-bearing chondrules examined contain olivine with undulose or mosaic extinction (deformation levels 2 and 3). No planar microfractures were seen in Chainpur olivine, despite experimental data which suggest that planar microfractures and undulose-mosaic extinction develop in olivine at similar shock pressures (*e.g.*, Müller and Hornemann, 1969; Bauer, 1979). No evidence for intense shock deformation of olivine (deformation level >3) was found (Fig. 4).

Two kinds of low-Ca pyroxene ($Fs_{1-25}Wo_{0.5-2}$) with different optical and microstructural properties are present in Chainpur chondrules. The most common kind is polysynthetically twinned on (100) and consists largely of the clinoenstatite (space group $P2_1/c$) polymorph (hereafter abbreviated as "CLEN") (Binns, 1967). Optical evidence for strain in such twinned pyroxenes, such as bent twins or undulose-mosaic extinction, is extremely rare in Chainpur.

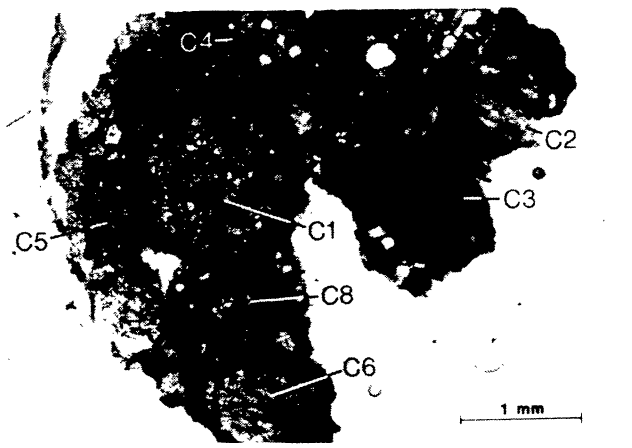

FIG. 2. Plane-polarized transmitted light micrograph of section C. All of the chondrules shown with designations in the figure were observed with TEM. A fine-grained "dark rim" surrounds C3. C1, C3 and C4 are droplet chondrules, C5 is a droplet chondrule fragment, and C2, C6 and C8 are irregular chondrules.

The second kind of pyroxene lacks polysynthetic twinning, although it sometimes shows diffuse lamellar banding under crossed-nicols. Remarkably, these "untwinned" pyroxenes *always* show undulose or mosaic extinction (mainly deformation levels 2 and 3) (Fig. 4). Both kinds of pyroxene often coexist in the same chondrules, but only the untwinned pyroxenes show obvious evidence for strain. Similarly, 30 chondrules contain both olivine and untwinned pyroxene phenocrysts, and deformation levels in untwinned pyroxene exceed those in olivine by at least one level in ~90% of these cases.

Untwinned pyroxene may generally correspond to the "striated pyroxene" described by other workers (Jobbins *et al.*, 1966; Binns, 1967, 1970). Striated pyroxene mainly consists of the orthoenstatite ("OREN"—space group Pbca) polymorph, but it contains numerous (100) lamellae comprised of CLEN (Ash-

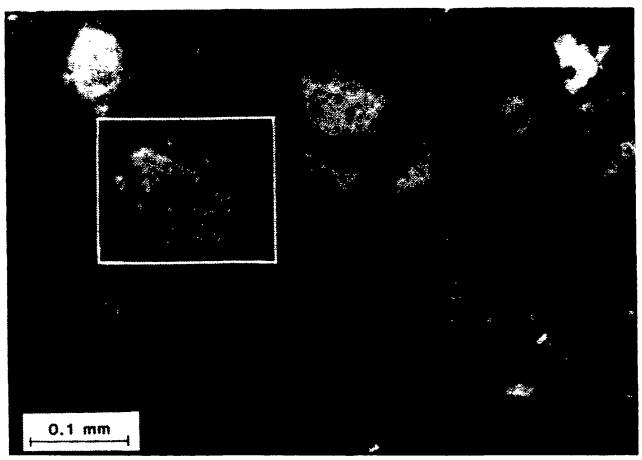

FIG. 3. Plane-polarized transmitted light micrograph of KA10, which contains olivine phenocrysts set in a groundmass of olivine and feldspar. The large olivine phenocryst within the boxed region appears euhedral in reflected light and shows a domain structure (subgrains) in transmitted light. TEM data suggest that these subgrains formed as a result of microstructural recovery during static annealing (see text).

TABLE 3. TEM olivine data.

Chondrule & grain type[1]		Dislocation density[2] (cm^{-2})	Area observed[3] (cm^2)
C1	igneous	$<1 \times 10^4$	2×10^{-3}
C1	dusty	$1–4 \times 10^8$	6×10^{-6}
C2	poikilitic	$\sim 1 \times 10^8$	1×10^{-6}
C4		$<1 \times 10^7$	6×10^{-6}
C6	poikilitic	$\leq 1 \times 10^7$	3×10^{-6}
C8		$2–3 \times 10^9$	2×10^{-5}
D2		$<1 \times 10^6$	2×10^{-5}
G1		$<1 \times 10^6$	5×10^{-5}
G5		$\leq 1 \times 10^5$	1×10^{-5}
KA1		$\leq 1 \times 10^7$	7×10^{-6}
KA10		5×10^7 to 1×10^8	1×10^{-4}
MA2	dusty	$\sim 5 \times 10^8$	1×10^{-6}

[1] Poikilitic = olivine completely enclosed within low-Ca pyroxene; igneous = euhedral-subhedral, normally zoned olivine; dusty = dusty-metal-bearing olivine.
[2] Determined by counting number of free dislocations in TEM micrographs; no correction made for foil thickness.
[3] Minimum area of electron-transparent olivine examined with TEM, estimated from micrographs of TEM mounts.

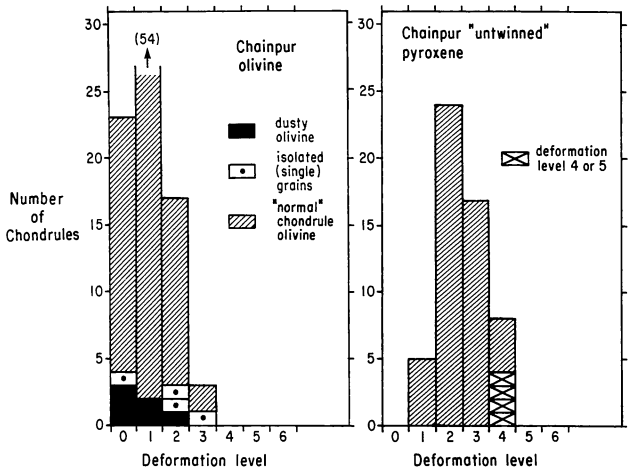

FIG. 4. Histograms summarizing the optical "deformation level" characteristics of olivine and low-Ca untwinned pyroxene from 90 olivine-bearing and 55 pyroxene-bearing chondrules and in 4 large isolated olivine grains in Chainpur. See Table 1 for criteria. Dusty-metal-bearing olivine was classified separately from "normal" or "igneous" olivine. Most olivine shows normal or barely perceptible undulose extinction whereas most untwinned pyroxene shows undulose-mosaic extinction.

worth, 1980). That untwinned pyroxene corresponds to striated pyroxene is suggested by the petrographic observations of Binns (1970, p. 664), who noted that the "striations" in striated pyroxene can appear to show "an undulose extinction if [observed] at low inclinations to the section."

Carraweena

Carraweena (L3) is a good example of a shocked Type 3 chondrite (Heymann, 1967; Carter *et al.*, 1968). This chondrite was examined to determine whether it too shows an apparent discordancy in strain between olivine and low-Ca pyroxene. Fifty chondrules in Carraweena were assigned deformation levels in exactly the same way as for Chainpur. Most of the pyroxene in Carraweena is optically untwinned, and unlike Chainpur, olivine and pyroxene in Carraweena show mutually consistent deformation levels (typically deformation levels 2–4). Many examples of planar microfractures and displacements across microfractures were noted in Carraweena olivine grains. Carraweena also contains abundant, interchondrule melt pockets. Taken together, these characteristics suggest a shock facies (Dodd and Jarosewich, 1979) of **d** or **e** for Carraweena.

Carraweena can be successfully described by the shock classification scheme, unlike Chainpur. It will be argued in this paper that low-Ca pyroxene grains in Chainpur chondrules are strained, but that this strain did not originate through impact shock.

Olivine Microstructures

Olivine in Chainpur chondrules typically contains a very low density of dislocations ($\leq 10^7$ cm^{-2} or even $<10^4$ cm^{-2}) (Table 3). C8 is an exception: it contains heavily deformed olivine and is discussed in detail later. Moderate dislocation densities ($\sim 1–5 \times 10^8$ cm^{-2}) are present in an olivine grain that is poikilitically enclosed by low-Ca pyroxene in C2, in two separate dusty-metal-bearing olivine grains ($\sim 100–300$ μm across) in C1, and in dusty-metal-bearing olivine in MA2 (Table 3).

Most of the dislocations in dusty-metal-bearing olivine grains are not spatially associated with metal or other inclusions (Fig. 5a). In C1, dislocations are absent in coexisting, normally-zoned and clearly "igneous" olivine phenocrysts (Table 3). This difference between "dusty" and "igneous" olivine in C1 is not related to the orientation of the grains or to their position in the chondrule, as at least two dozen igneous olivine grains, each with a different orientation and at widely separated positions, were observed with TEM in C1.

The configuration of dislocations in olivine varies from chondrule to chondrule and can be used as a probe of annealing histories. Annealing is manifested by microstructural recovery, which entails the climb of dislocations out of slip planes; for olivine this has been shown to result in curved dislocations, dislocation loops, and subgrain boundaries (Phakey *et al.*, 1972; Goetze and Kohlstedt, 1973; Ashworth and Mallinson, 1985). Dislocations are straight and unassociated with subgrain boundaries in C2 olivine, whereas in KA1, all dislocations are present in subgrain boundaries. In olivine from KA10, most dislocations are curved or contained in arrays of subgrain boundaries (Fig. 5b), and several dislocation loops (~ 0.2 μm diameter) were found. Dusty-metal-bearing olivine grains from C1 and MA2 contain curved dislocations and some subgrain boundaries.

→

FIG. 5. TEM bright field micrographs illustrating microstructures in Chainpur chondrules. (a) Typical view of scattered dislocations in dusty-metal-bearing olivine, C1. The faint splotches are surface contamination introduced during ion-milling. (b) Subgrain boundary in olivine, KA10. (c) Equigranular olivine grains meet in triple junctions (T), KA10. A small amount of glass and crystalline material (chondrule groundmass) intervenes between some of the olivine grains. The bright area at upper left is a void produced during ion-milling. (d) Multiple fine-scale (100) lamellae in low-Ca pyroxene, from the "dark rim" of C3. A healed microcrack (M-M) is crossed by some but not all of the lamellae. (e) Low-Ca pyroxene nearly devoid of (100) lamellae, C4. Both unit (U) and partial (P) dislocations are present, but only the former are in contrast. The

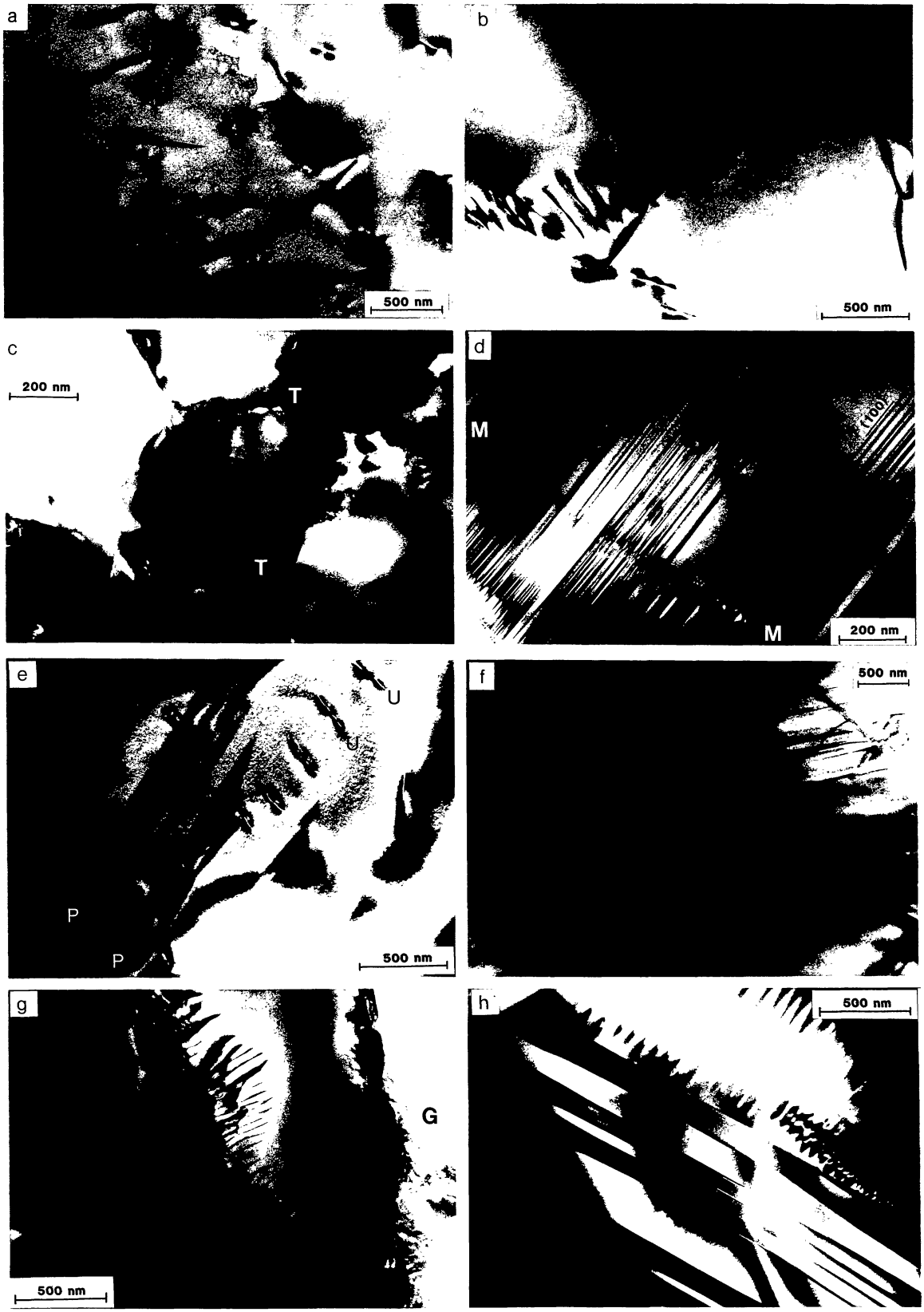

partial dislocations occur at the ends of (100) stacking faults, which here appear as diffuse, striped bands. (f) Numerous unit dislocations in low-Ca pyroxene comprised predominantly of the OREN polytype, C2. (g) Subgrain boundaries in high-Ca pyroxene (Al-diopside), C4. Chondrule groundmass (G) is at extreme right. (h) Polysynthetic twins in Na-rich feldspar, KA10. The feldspar contains exsolution lamellae near one of its margins (upper right).

In some areas within KA10, small equigranular olivine grains are in close proximity to one another and meet in triple junctions (Fig. 5c). A minute amount of quartzofeldspathic glass, probably residual melt, intervenes between some of the equigranular olivine grains. The triple junctions and equigranular texture suggest the approach to an equilibrium state in which interfacial strain energies are minimized (Ragan, 1969). This texture probably formed as a result of static annealing.

Low-Ca Pyroxene Microstructures

The most common defects in low-Ca pyroxene from Chainpur chondrules are (100) microstructures that represent stacking faults (planar interfaces that separate pyroxene with the OREN and CLEN polytypes) and microtwins (small-scale twins). The (100) microstructures are here termed "lamellae" because of their appearance in TEM bright field images (Fig. 5d). In general, the (100) lamellae are distributed non-uniformly throughout low-Ca pyroxene grains within a given chondrule. This heterogeneity is partly an intra-grain phenomenon, but in some chondrules (as in C2), different grains contain distinctly different densities of (100) lamellae.

(100) stacking faults and microtwins entail coherent interfaces and so do not impart any strain to the pyroxene lattice (Buseck *et al.,* 1980). However, low-Ca pyroxene grains in Chainpur chondrules also contain unit dislocations, partial dislocations, and both open and healed microcracks—features that testify to the presence of strain in these pyroxenes. The degree of strain in low-Ca pyroxene varies from chondrule to chondrule and from grain to grain, but all chondrules contain some pyroxenes that are at least slightly strained. It should be emphasized that this is true even when accompanying olivine in the chondrules shows no defects whatsoever (as in C4).

Partial dislocations are common in both optically twinned and untwinned pyroxene and indicate that many of the (100) lamellae are stacking faults (Fig. 5e). Unit dislocations primarily occur in areas with few lamellae (Figs. 5e–f) and locally attain maximum densities of $\sim 5 \times 10^8$ cm^{-2}. These dislocations are often curved, suggesting recovery. In C2, one large (180 × 700 μm), optically untwinned pyroxene is comprised mainly of OREN and shows mosaic extinction. This grain contains numerous unit dislocations and few lamellae (Fig. 5f), whereas optically twinned pyroxenes in the chondrule contain few unit dislocations and numerous (100) lamellae. These observations provide evidence for a difference in the microstructures between optically twinned and untwinned low-Ca pyroxene.

Open and healed microcracks (Fig. 5d), and 50–700 nm-wide "veinlets" comprised of Si- and Al-rich glass and fine-grained material (quartzofeldspathic groundmass), are common in both optically twinned and untwinned pyroxene grains. Microcracks and veinlets preferentially occur at high angles (often nearly perpendicular) to (100) of the host, although they are sometimes parallel to (100). Figure 5d shows an example of how some lamellae originate at a healed microcrack while others appear to cross over it unimpeded. In many cases, low-Ca pyroxene is crystallographically misoriented and locally strained in the vicinity of open and healed microcracks, suggesting that crack formation involved straining of the pyroxene lattice. Veinlets perpendicular to (100) in the large, untwinned pyroxene in C2 have ragged, opposing margins that appear as if they once fitted together. This suggests that the glassy veinlets originated as microcracks that were subsequently filled with groundmass material, possibly residual chondrule melt.

High-Ca Pyroxene Microstructures

Three chondrules (C1, D2, G1) contain numerous groundmass pyroxenes that show fine-scale exsolution between diopsidic and magnesian low-Ca endmembers. The fine exsolution appears as diffuse modulated microstructures characteristic of spinodal decomposition, suggesting formation under conditions of relatively rapid cooling (Champness and Lorimer, 1976; Buseck *et al.,* 1980). Similar finely exsolved pyroxenes are common in droplet chondrules from Type 3 ordinary and carbonaceous chondrites (Ashworth and Barber, 1977; Töpel-Schadt and Müller, 1985).

Augite epitaxially overgrows low-Ca pyroxene in C4 and occurs at the margins of olivine phenocrysts in KA1. In C4, the augite is itself overgrown by an aluminous clinopyroxene. The augite and Al-clinopyroxene in C4 and KA1 lack exsolution lamellae but contain subgrain boundaries (Fig. 5g), and in this way resemble diopsidic pyroxene in Quenggouk (H4) and Allegan (H5) (Ashworth, 1981). The presence of subgrain boundaries in overgrowths from KA1 and C4 implies that these two chondrules were at least partially annealed at a relatively late-stage, after most of the olivine and pyroxene in them had crystallized.

Mesostases

Quartzofeldspathic glass is present in all chondrules that were observed with TEM, but the proportion of such glass to crystalline phases in mesostases varies considerably from object to object. At one extreme, C1, D2 and G1 contain abundant Na-Al-Si-rich glass. At the other extreme, the mesostases of KA1 and KA10 contain little glass and instead contain abundant plagioclase feldspar (Fig. 5h). The feldspars (typically 1–3 μm across) are polysynthetically twinned and lack dislocations. They are Na-rich (Na $\gg$ Ca > K), corresponding certainly to $Ab_{>80}$ and probably to Ab_{90-100}. Feldspar poikilitically encloses small (~0.07–0.4 μm-diameter) equant olivine grains in some areas within KA10, and in KA1 it encloses augite.

Chondrule C8

The only chondrule observed with TEM that shows good evidence for significant impact shock is C8, an olivine-pyroxene microporphyry with an irregular form (Fig. 6a). The largest olivine (~120 μm across) in C8 has a dusty (~50 μm diameter) core that contains numerous inclusions of chromite (as identified with the microprobe) (Fig. 6a). Such dusty-chromite-bearing olivine grains may be relict (Christophe Michel-Lévy, 1981, p. 75; Watanabe *et al.,* 1984), analogous to dusty-metal-bearing olivine. The few olivines and pyroxenes in C8 sufficiently coarse for thin-section study show uniform and undulose extinction, respectively. However, following ion-milling of C8, the dusty olivine appeared optically to consist of four roughly equidimensional regions of differing orientation.

Low-Ca pyroxenes in C8 exhibit relatively few and non-uniformly distributed (100) lamellae, some partial dislocations, and numerous unit dislocations and microcracks. Many of the unit dislocations are curved. Only limited TEM observations were performed on the margin of the large (and possibly relict) olivine grain, but good TEM observations of olivine in the groundmass

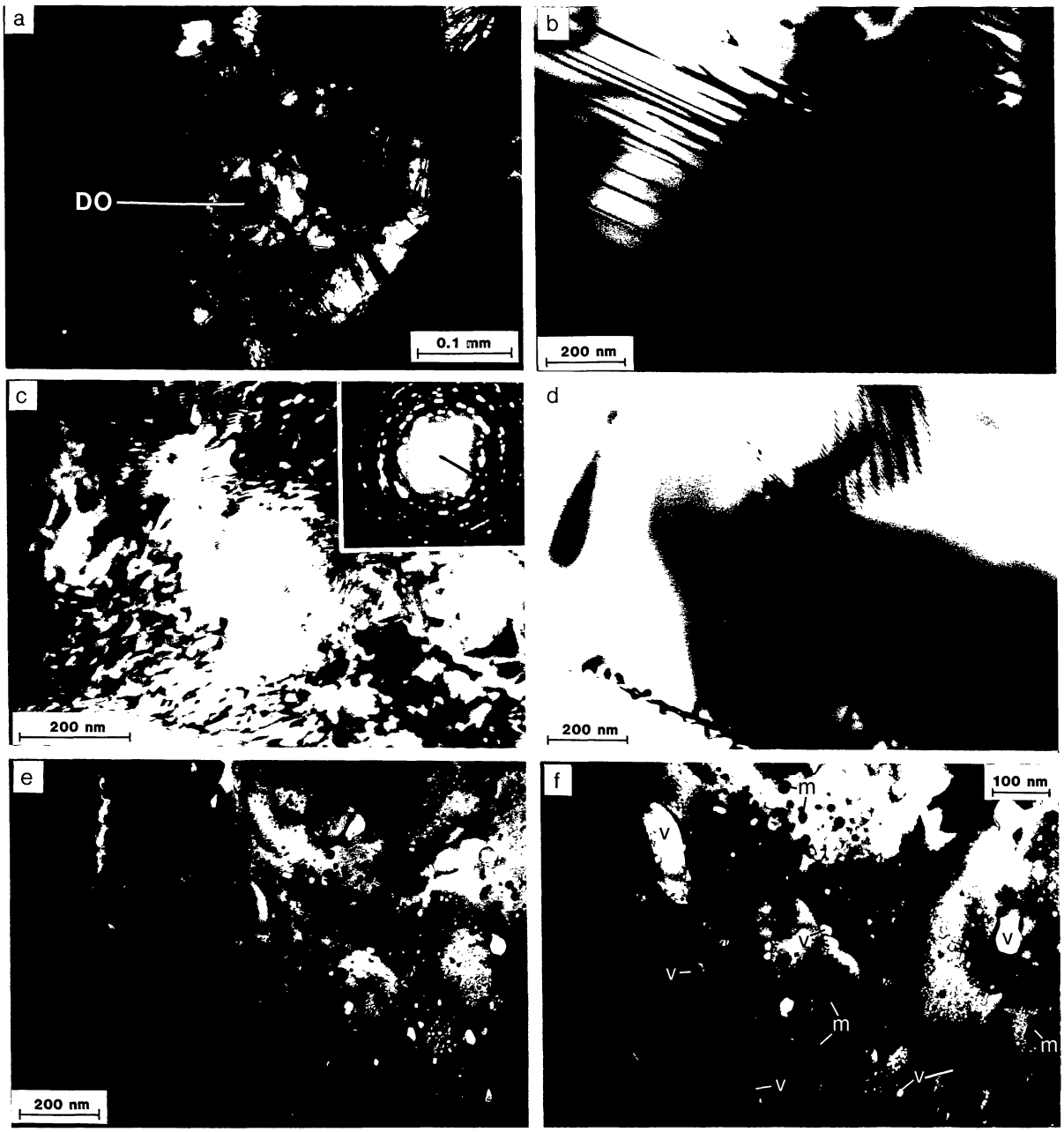

FIG. 6. Chondrule C8. (a) Cross-polarized transmitted light micrograph of C8, which contains olivine and optically untwinned, low-Ca pyroxene set in a fine-grained (<20 μm) groundmass of the same minerals. The largest olivine grain (DO) contains a dusty core rich in chromite inclusions. (b) TEM micrograph of olivine, showing dislocations grading into a more heavily deformed area at right. (c) TEM micrograph of deformed olivine that exhibits small-scale contrast variations produced by intense strain. Inset: accompanying electron diffraction pattern showing the elongation and smearing of diffraction spots into arcs, indicating lattice strain. (d) TEM micrograph of subgrains in olivine. This texture formed by recrystallization or extensive recovery. (e) TEM micrograph of the contact between void- and inclusion-rich olivine (right) and intensely deformed olivine (left). The void- and inclusion-rich olivine completely lacks dislocations and is interpreted to be the product of a shock melt. (f) Higher magnification view of the inferred shock melt zone in C8 showing voids (v) and Ni-Fe metal inclusions (m).

of C8 were obtained. Microcracks are rare in the groundmass olivines, but dislocations are common and have a typical density of 2–3 $\times$ 10^9 cm^{-2}. Although numerous straight dislocations are present in some areas (Fig. 6b), highly curved dislocations occur in areas of lower dislocation density (~5 $\times$ 10^8 cm^{-2}), consistent with localized recovery. The most intensely deformed olivine in C8 shows small-scale contrast variations arising from extreme lattice strain and is so heavily deformed that individual dislocations are difficult to discern (Fig. 6c).

In some areas within C8, olivine is free of defects except for narrow, well-formed subgrain boundaries (Fig. 6d). This microstructure could have formed through solid-state recrystallization or an advanced stage of recovery. The former possibility is more likely for C8, as the individual subgrains often differ

significantly from one another in their orientations, and the virtually unstrained olivines occur amidst heavily deformed olivine, two characteristics more consistent with recrystallization than with recovery (Hull, 1975; Lally *et al.,* 1976; Christie and Ardell, 1976).

A feature in C8 unique among the chondrules observed with TEM is the presence of olivine that contains numerous voids (~10–100 nm across) and crystalline inclusions (up to ~50 nm across). The olivine is free of dislocations in the area containing the highest number of voids but grades into heavily deformed olivine over a distance of ~0.1–0.5 μm (Fig. 6e).

Based on AEM analyses many of the crystalline inclusions appear to be Ni-rich (Fe:Ni ~ 2:1) metal. The high Ni content of the metal inclusions is unlike that of the much coarser (~1 μm-diameter), Ni-poor (<0.1 wt.%) metal inclusions typical for dusty olivine (Rambaldi and Wasson, 1982), suggesting that the two types of metal have different origins. Sulfur was detected in the vicinity of some of the crystalline inclusions, implying that additional phases (sulfides?) may also be present. The host olivine appears to be more fayalitic than elsewhere in the chondrule, but this may be an artifact caused by inadvertent x-ray excitation of the inclusions.

The smallest voids are clearly embedded within olivine (Figs. 6e–f) and so cannot be an artifact of sample preparation; many of these voids have straight margins suggesting crystallographic control of their boundaries. Some voids have smoothly curving margins and comprise spherical, elongate, or dumbbell-shaped cavities (Figs. 6e–f).

DISCUSSION

Correspondence between Optical and TEM Techniques

This work is one of the first to utilize both optical and TEM methods for the study of individual chondrules, and it is thus appropriate to evaluate how well the two methods correspond.

It appears that great care must be exercised in using optical data to constrain the shock histories of individual chondrules. For instance, apparent discrepancies between optical and TEM data are suggested for olivine in chondrules G5 and C8. In the former case, TEM showed olivine to be nearly undeformed, although it exhibited pronounced mosaic extinction; in the latter case, TEM showed groundmass olivine to be heavily deformed, while a few coarse olivine grains in the chondrule exhibited uniform extinction. Two different explanations for these apparent discrepancies seem likely. For G5 olivine, crystallographic misorientation across widely-separated subgrain boundaries can explain its apparent mosaic extinction. For C8, little coarse (>20–30 μm) olivine is present and the largest grain contains numerous dusty inclusions, making a reliable assessment of strain levels in these grains difficult.

Such discrepancies notwithstanding, both optical and TEM data are in agreement concerning the *typical* levels of strain in olivine and pyroxene from Chainpur chondrules. Both data sets suggest that olivine is usually nearly undeformed and that low-Ca pyroxene is usually strained, and that optically untwinned pyroxene grains are more heavily strained than polysynthetically twinned pyroxene grains.

Significance of Strain in low-Ca Pyroxene

Optical and electron microscope observations of Chainpur chondrules suggest that low-Ca pyroxenes are often strained, but that most olivine is essentially undeformed. This discordancy can be explained in four ways: 1) chondrules were lightly shocked and pyroxene is a more sensitive indicator of shock than olivine; 2) chondrules were intensely shocked and olivine preferentially melted; 3) chondrules were shocked and subsequently annealed, and olivine experienced preferential removal of dislocations through recovery or recrystallization; or 4) impact shock was not responsible for straining pyroxene grains in Chainpur chondrules.

The first possibility, that pyroxene is a sensitive indicator of shock, is contrary to the conclusions of several researchers (Carter *et al.,* 1968; Christie and Ardell, 1976), who found that pyroxene is generally less, rather than more, susceptible to plastic deformation than olivine. Preferential melting of olivine during intense shock episodes is also untenable, because experimental shock loading of both particulate and rock targets show that pyroxene is more readily shock-melted than olivine (Schaal and Hörz, 1977; Schaal *et al.,* 1979; Bauer, 1979). Preferential removal of dislocations in olivine by recovery also cannot easily explain the data, as annihilation of dislocations by recovery is quantitatively unimportant (Goetze and Kohlstedt, 1973). Finally, preferential recrystallization of olivine should have produced a distinctive subgrain (domain) microtexture in this mineral (*cf.* Lally *et al.,* 1976), which is absent in most chondrules.

It thus appears that strain in chondrule pyroxene often originated in a process other than shock. A similar conclusion was reached for lunar pigeonites and augites in Apollo 11 basalts (Carter *et al.,* 1970; Sclar, 1970; Chao *et al.,* 1970). As discussed below, low-Ca pyroxene in Chainpur chondrules was probably strained by polytype transformations (protoenstatite → CLEN/OREN and CLEN → OREN) that arose during the crystallization and annealing of the chondrules.

Microcracks and veinlets roughly perpendicular to (100) of low-Ca pyroxene have been attributed to the inversion of protoenstatite ("PEN"—space group Pbcn) to CLEN or a CLEN/OREN mixture (Binns, 1970; Kitamura *et al.,* 1983; Yasuda *et al.,* 1983), as this inversion entails ~2% shortening parallel to the c-axis of pyroxene (Smyth, 1974; Cameron and Papike, 1980). The 1-bar stability field of PEN probably extends to compositions as ferrous as Fs_{20} (Huebner, 1980; Biggar, 1986) and encompasses the composition for most low-Ca pyroxene in Chainpur, which is consistent with the idea that PEN was initially present in most Chainpur chondrules. In Chainpur, microcracking of low-Ca pyroxene was accompanied by straining of the pyroxene lattice, and some microcracks may have been filled with residual chondrule liquids. The latter observation suggests that the PEN → CLEN or PEN → CLEN/OREN inversion occurred above the solidus in these chondrules (Yasuda *et al.,* 1983).

The presence of unit dislocations and an uneven distribution of (100) lamellae in low-Ca pyroxene from Chainpur can be explained by shock deformation (Heuer *et al.,* 1974; Sears *et al.,* 1984) or by the growth of OREN at the expense of CLEN during annealing (Coe and Kirby, 1975). For Chainpur chondrules, the second possibility is more likely. Coe and Kirby (1975) demonstrated experimentally that (100) lamellae are destroyed and that numerous unit dislocations are produced by the CLEN → OREN transition during annealing. This would explain the tendency in Chainpur pyroxene for unit dislocations to occur in areas with few (100) lamellae. Moreover, the CLEN → OREN inversion requires annealing and is therefore consis-

tent with evidence for recovery (curved unit dislocations) in low-Ca pyroxene. Finally, the coexistence of both optically twinned (CLEN-rich) and untwinned (probably more OREN-rich) pyroxene grains in chondrules can also be explained by the CLEN → OREN inversion, because the degree of impingement of crystals upon one another could provide local barriers to shape-change (Ashworth, 1980), thereby allowing some grains to invert more than others within a given chondrule.

It should be noted that in the experiments of Coe and Kirby (1975), CLEN was initially produced by shear deformation of OREN, and thus during subsequent annealing, CLEN reverted to OREN. However, this does not necessarily imply that CLEN in Chainpur chondrules was initially produced from OREN by deformation, because according to Ashworth (1980, p. 174), reversion *or* inversion of CLEN to OREN should result in similar microstructures, so long as CLEN was not initially twinned on a fine scale (Ashworth *et al.,* 1984).

Deformation of Relict (Dusty) Olivine Grains

This work raises the number of dusty olivine grains observed with TEM to four, including three separate dusty-metal-bearing grains in C1 and MA2, and one dusty-chromite-bearing olivine in ALHA-77015 (L3) described by Watanabe *et al.* (1984). In every case the grains contain an appreciable number of dislocations, suggesting that dislocations are characteristic of dusty metal- and chromite-bearing olivine grains. This is potentially significant, for such dusty olivine grains probably survived the last episode of melting in their host objects. In C1, only the dusty (and not the igneous) olivine grains are deformed, strongly suggesting that the dislocations in the dusty olivine grains formed prior to the crystallization of igneous olivine in the chondrule (and thus before or during chondrule formation). Watanabe *et al.* (1984) reached a similar conclusion for the grain they studied.

Watanabe *et al.* (1984) found a high density of dislocations ($\sim 10^9$ cm^{-2}) in their grain, and attributed this to impact deformation. A similar origin may be invoked for the dusty olivine grains in Chainpur, but the evidence for this is equivocal. Moderate densities of free dislocations ($\sim 10^8$ cm^{-2}) in olivine, such as are found in the dusty olivine grains in Chainpur, can be produced by stresses generated during the exsolution of metal or pyroxene from olivine during reduction (Boland and Duba, 1981). Stresses arising through exsolution can produce dislocations in olivine that are not spatially associated with the exsolved inclusions themselves (Boland and Duba, 1981), as in Chainpur. Although Burgers vector determinations for dislocations were not carried out in the present study, dislocations with **b** = [001] and **b** = [100] are characteristic of both experimentally-reduced olivine (Boland and Duba, 1981) and the grain examined by Watanabe *et al.* (1984). Thus, it may be difficult to determine whether dislocations in dusty olivine grains originated through impact shock or exsolution-reduction. It is also possible that thermally-induced stresses generated during chondrule formation could introduce dislocations in relict or xenocrystic olivine, in a process analogous to thermal fatigue (Levi, 1973).

Shock Metamorphism and Melting of C8

Among the 14 chondrules in Chainpur investigated with TEM, only C8 shows evidence for significant impact shock. The high density of dislocations in olivine from this chondrule is a feature that typifies impact shock in meteorites (Ashworth and Barber, 1975; Ashworth, 1985). Evidence for localized annealing in C8 (curved dislocations in olivine and low-Ca pyroxene) is consistent with the transient high temperatures that could have accompanied a shock event. The well-developed subgrain texture found in some places within C8 (Fig. 6d) resembles recrystallized olivine in the intensely shock-metamorphosed Wickenburg (L6f) chondrite (Ashworth, 1985).

The complete lack of dislocations in the void- and metal-inclusion-rich olivine in C8, the proximity of this olivine to an intensely deformed area, and the presence of voids are consistent with the idea that this olivine crystallized from a shock melt. The numerous voids suggest that the shock melt crystallized rapidly, thereby trapping vapor that was generated during impact. The voids often appear to outline regions of olivine (~0.1–0.3 μm across) that have slightly differing crystallographic orientations (Fig. 6e); this could be interpreted as the incipient segregation of the olivine into separate grains of this size. The inferred shock-melt zone in C8 is strikingly similar to "crystalline melt pockets" that contain olivine, voids and Ni-bearing metal inclusions in the intensely shocked Taiban (L5e) meteorite (Ashworth, 1985). This similarity supports the interpretation that C8 was shock-melted.

Shock pressures of ~10–50 GPa are required for significant plastic deformation of olivine (Reimold and Stöffler, 1978; Bauer, 1979; Stöffler *et al.,* 1988), and shock pressures >20 GPa are needed for the incipient shock melting of particulate olivine (Bauer, 1979) and bulk chondrites (Stöffler *et al.,* 1988). By comparison, incipient shock melting of a "massive" dunite target requires shock pressures >60–75 GPa (Reimold and Stöffler, 1978; Bauer, 1979), which is too high to be consistent with the preservation of large areas of unannealed, heavily deformed olivine in C8. It therefore appears that the equilibrium shock pressure within C8 reached ~20–50 GPa, which corresponds to a shock facies of **d** or **e** (Stöffler *et al.,* 1988).

Although C8 was strongly shocked, olivine in neighboring chondrules is virtually undeformed, except for dusty-metal-bearing olivine grains in C1 and a poikilitic olivine grain in C2. It is very unlikely that C8 could have been shocked *in situ.* C8 was almost certainly shocked prior to the final agglomeration of Chainpur, either while the chondrule was an independent entity in space, or while it was in a parent body.

The near-absence of recognizable agglutinates in chondrites suggests that most chondrules did not form by shock melting in a regolith (Kerridge and Kieffer, 1977). However, this does not rule out the possibility that some chondrules, such as C8, were shocked in a regolith.

A Shock-Melt Origin for Chondrules?

The severity with which chondrule C8 was shocked, and especially the evidence for localized impact-melting of olivine within it, suggests that *some* chondrules may have formed by shock melting. The presence of dislocations in dusty olivine grains, which *may* have formed by impact deformation during chondrule formation (see above), is consistent with this idea.

Based on optical and TEM data for olivine, it seems clear that relatively few chondrules (<15%) in Chainpur were shocked to pressures above ~5–10 GPa *after* chondrule formation. If chondrules *formed* by shock melting, then the data for Chainpur imply that the precursors must have been extensively melted, so as to obliterate evidence for deformation. Indeed, Dodd (1978b, 1982) and Dodd and Jarosewich (1979) noted that near-

TABLE 4. Summary of TEM observations pertinent to the thermal histories of Chainpur chondrules. Abbreviations as in Table 2.

Object	Olivine	Low-Ca pyroxene	High-Ca pyroxene	Comments and inferences
C1	curved disloc. + subgrain boundaries in dusty ol only	—	spinodal decomposition	abundant glass; late-solidifying phases cooled rapidly, but dusty ol annealed
C2	straight dislocations; one healed microcrack	tpx mainly lamellar; curved unit + rare disloc. loops in upx	—	upx shows good evidence for annealing
C3	—	lamellae + curved unit disloc.; fine lamellae in rim	—	—
C4	—	lamellae + curved unit dislocations	subgrain boundaries in overgrowths	chondrule (especially late-crystallizing phases) annealed
C5	—	mainly (100) lamellae	—	rapid cooling?
C6	—	mainly (100) lamellae in chondrule core	—	rapid cooling for core of chondrule?
C8	locally: curved disloc. + subgrain boundaries	lamellae + curved unit dislocations	—	transient heating accompanied intense shock
D2	—	—	spinodal decomposition	abundant glass; late-solidifying phases cooled rapidly
G1	—	—	spinodal decomposition	abundant glass; late-solidifying phases cooled rapidly
G5	1 well-defined subgrain boundaries	—	—	—
G6	—	curved unit dislocations	—	upx shows evidence for annealing
KA1	all disloc. in subgrain boundaries	lamellae + subgrain boundaries	subgrain boundaries in overgrowths	little glass, abundant plagioclase; chondrule extensively annealed
KA10	curved disloc. + disloc. loops + subgrain boundaries	—	—	little glass, abundant plagioclase; chondrule extensively annealed
MA2	curved disloc. + subgrain boundaries	—	—	dusty ol annealed

ly complete shock melting of chondrules would be required to explain the bulk chemical variations of chondrules. Nearly complete impact-induced melting of olivine and pyroxene requires shock pressures >80–85 GPa (Schaal and Hörz, 1977; Schaal *et al.*, 1979; Bauer, 1979).

While it is conceivable that most chondrules formed by shock melting and that few chondrules were subsequently affected by significant impact deformation, this does not seem very likely. The apparent dearth of chondrules in Chainpur shocked to pressures between ~5–10 GPa and ~80–85 GPa appears to be at odds with the supposition that the chondrules (or their precursors) were first subjected to extensive shock melting, because it implies an unreasonably abrupt cessation in the importance of shock processes immediately after most chondrules formed. For this reason, a shock melt origin for *most* chondrules is not favored.

Annealing of Chondrules

Based on a variety of microstructures (summarized in Table 4), Chainpur chondrules appear to have been affected by various degrees of annealing. As only chondrule C8 shows persuasive evidence for shock (see above), there is no reason to believe that the annealing of other chondrules arose during shock-heating; instead, the annealing apparently reflects thermal metamorphism (static heating).

Annealing was most extensive for chondrule KA1, which contains "equilibrated" olivine of LL4 composition. It is the only chondrule investigated with TEM in which subgrain boundaries occur in three phases—olivine, low-Ca pyroxene and high-Ca pyroxene (augite). The augite in this chondrule, and in C4, is microstructurally similar to diopside in equilibrated chondrites (Ashworth, 1981). Little glass is present in KA1, but feldspar is abundant. Chondrule KA10 was also extensively annealed. It is the only chondrule in which dislocation loops were found in olivine, and the only one besides KA1 in which feldspar is abundant.

Other chondrules in Chainpur appear to have cooled rapidly. Spinodal decomposition textures in groundmass high-Ca pyroxenes and abundant glass in C1, D2 and G1 imply rapid cooling during the late-stage igneous crystallization and solidification of these chondrules, and a lack of appreciable reheating. Low-Ca pyroxene in C5 and in the core of C6 are microstructurally lamellar and lack curved unit dislocations, which could indicate that these chondrules cooled quickly and were not significantly reheated.

During annealing of olivine the proportion of dislocations that are free (unassociated with subgrain boundaries) to those that are bound in subgrain boundaries decreases with an increase in temperature or duration of heating (Goetze and Kohlstedt, 1973). The bound/free ratio of dislocations in Chainpur olivine increases in the sequence: C2 < C1 dusty ~ MA2 dusty < KA10 < KA1, which implies the least amount of annealing for C2 and the most for KA1. Dusty-metal-bearing olivine grains were probably annealed at the time of chondrule formation when temperatures were highest; as noted above, C1 was cooling rapidly at lower (near-solidus or subsolidus) temperatures.

Among the five droplet chondrules and one droplet fragment chondrule studied with TEM, all but two of the droplet chondrules were minimally annealed. KA1, KA10 and G6, all irregular chondrules, experienced considerable annealing. Other irregular chondrules either provide inconclusive evidence for annealing or show some evidence for annealing. It thus seems, based on the small number of chondrules examined, that irregular chondrules experienced more annealing than droplet chon-

drules or droplet fragments. The correlation between form and annealing history is not rigorous, as at least one droplet chondrule (C4) shows good evidence for annealing.

There also appears to be a weak correlation between the overall FeO/MgO ratio of chondrules and their extent of annealing, if one excludes MA2, which is mainly comprised of dusty-metal-bearing olivine. The most rapidly cooled chondrules (C1, D2, G1) contain highly forsteritic olivine (Fa_{0-5}), while more annealed chondrules (C2, C4, G6, KA1, KA10) contain relatively ferrous olivine (Fa_{14-34}) and pyroxene (Fs_{8-26}). However, not all ferrous chondrules show obvious evidence for annealing. It is clear that annealing is *not* directly correlated with the mean CaO content of olivine, supporting the conclusions of Lofgren (1985), although such a correlation was expected based on earlier work (*e.g.,* Dodd, 1972, 1973; Steele and Smith, 1975).

Other data support the inference that, in general, annealing was more extensive for high-FeO and irregular chondrules than for low-FeO and droplet chondrules. TEM observations suggest that the optically visible subgrains in olivine phenocrysts from KA10 (Fig. 3) formed by microstructural recovery during annealing. Similar features in three additional olivine microporphyries (Al, IB4, KB9) and four microgranular pyroxene chondrules (KA14, KA18, KA19, MA14) not studied with TEM may have formed in the same way. Of these seven chondrules, six have an irregular form and only one (A1) is a droplet chondrule. Moreover, at least five of these chondrules also contain relatively ferrous silicates (Fa_{15-40}, Fs_{10-22}). (Mineral compositions were not determined for MA14, and KA14 contains somewhat more magnesian pyroxene, Fs_{6-8}.)

The variability in the thermal histories of chondrules can only be explained if they were annealed to different degrees before the final agglomeration of Chainpur. This leaves open the possibility of thermal metamorphism occurring during: 1) sufficiently slow cooling from melt temperatures (by autometamorphism); or 2) reheating.

Optical and TEM data cannot be used to rule out either of these possibilities. Based on the Goetze and Kohlstedt (1973) values for diffusivity in olivine, one can easily reconcile the observed microstructures in olivine indicative of recovery with moderately slow cooling (~100 °C/hr) over the temperature interval of ~1000–1500 °C. Such cooling rates are consistent with the slowest cooling rates inferred for microporphyritic chondrules (*e.g.,* Hewins, 1988), implying that autometamorphism may be a viable process. However, it is unclear whether these cooling rates can also be reconciled with evidence for microstructural recovery and the CLEN → OREN transformation in pyroxene from Chainpur chondrules, or whether reheating is required.

Processing of Chondrules during Accretion or in a Regolith

The data presented here suggest that Chainpur is an agglomerate or breccia whose individual constituents were physically mixed or reworked on a millimeter-to-submillimeter scale, allowing chondrules of diverse histories to become juxtaposed. This conclusion is consistent with the results of other researchers for various Type 3 chondrites (see Introduction). The components of many Type 3 ordinary and carbonaceous chondrites may have been reworked during the accretion and disruption of their respective parent bodies, or during impact gardening of the regoliths on their respective parent bodies (see Bunch and Rajan, 1988, and references therein). Regolith activity has recently been suggested as the likely explanation for a 50 Myr time span in I-Xe ages of Chainpur chondrules (Swindle *et al.,* 1989).

The form of irregular chondrules implies that these chondrules may have been physically processed. For example, irregular chondrules may have formed through the brecciation of initially more extensive igneous rocks (Dodd, 1978a,b, 1981, p. 116), through the abrasion and fracturing of droplet chondrules (Christophe Michel-Lévy, 1981; Wlotzka, 1983), or through the co-aggregation of hot (and consequently somewhat plastic) chondrules with matrix-like material (Hutchinson and Bevan, 1983). These processes may have occurred during the accretion and disruption of parent bodies or the gardening of parent body regoliths, at the same time the components of Type 3 chondrites were being physically mixed.

It should be noted that Nagahara (1983) attributed the difference between irregular and droplet chondrules to the extent to which precursors were melted, with incomplete melting for irregular chondrules and more complete melting for droplet chondrules. However, most chondrules are inferred to have been heated to about the same peak temperature (Hewins, 1988), and in Chainpur, there is no evidence that relict grains are more abundant in irregular chondrules than in droplet chondrules. This suggests that chondrule form was not governed by the extent of melting of chondrule precursors.

Most chondrules in Chainpur were minimally affected by impact deformation, which argues against vigorous impact-stirring of a parent body regolith. If these chondrules were physically processed in a regolith, then this processing must have been relatively gentle. Moreover, the final accumulation process that brought chondrules in Chainpur together must have involved fairly low-velocity collisions.

Low-*g* objects, such as asteroids, are the likely parent bodies of meteorites. Such objects may have experienced considerable impact-induced seismic shaking (Cintala *et al.,* 1979; Hörz and Schaal, 1981), which could have led to a relatively gentle stirring of their regoliths. Alternatively, low-velocity collisions between planetesimals during the accretion (and possible reassembly following catastrophic break-up) of chondrite parent bodies (*e.g.,* Bunch and Rajan, 1988) would lead to a large ratio of displaced and weakly shocked material to heavily shocked material (Stöffler *et al.,* 1988), consistent with the data for Chainpur.

The apparent correlation between the form and annealing histories of chondrules in Chainpur may indicate that irregular chondrules were subjected to concurrent physical and thermal processing. However, it seems unlikely that the heat source for the annealing of Chainpur chondrules was provided by impact. The paucity of shock effects in most chondrules, the lack of an obvious correlation between annealing and shock-deformation, and the tendency for thermal effects of shock to become important only at high shock pressures (Bauer, 1979; Ashworth, 1985; Stöffler *et al.,* 1988) all argue against shock-induced annealing. Chondrules may have been autometamorphosed, in which case the heat source for annealing was provided by the (unknown) process that formed chondrules in the first place. Alternatively, if chondrules were annealed by reheating and cooled in a regolith, then the heat source for annealing could have been provided by interior warming of the parent body,

perhaps through the decay of radioactive ^{26}Al or through electrical induction heating.

CONCLUSIONS

The results of this study leave little doubt that chondrules in Chainpur experienced varied degrees of annealing and deformation. Chainpur may be regarded as an agglomerate or breccia that experienced little overall deformation or heating during and after the final accumulation and compaction of its constituents.

Most (probably >85%) of the chondrules in Chainpur were not significantly affected by impact-shock subsequent to their formation, based on the optical and microstructural properties of olivine. However, one microporphyritic chondrule shows good evidence for having been shocked to pressures of 20–50 GPa, prior to the final agglomeration of Chainpur. The existence of this chondrule strongly suggests that hypervelocity impact processes played a role in the early (pre-agglomeration) evolution of chondritic material. Some, but probably not most, chondrules may have formed by shock melting, and impact processes may have been responsible for abrading, fracturing and physically mixing chondrules during parent body break-up or regolith gardening.

Although most olivine in Chainpur chondrules shows little evidence for deformation or strain, low-Ca pyroxene grains—especially optically untwinned grains—are often strained. This strain is attributed to polytype inversions (PEN → CLEN/OREN and CLEN → OREN) that occurred during the igneous crystallization and static annealing of chondrules.

Moderate dislocation densities ($\sim 10^8$ cm^{-2}) are characteristic of dusty-metal-bearing olivine grains in chondrules. These dislocations were introduced before the crystallization of olivine phenocrysts in at least one chondrule. Dusty-metal-bearing olivine grains may have been strained by a reduction-exsolution process during chondrule formation, by thermal stresses associated with chondrule formation, or by impact deformation before or during chondrule formation.

Some chondrules, especially droplet chondrules containing glassy mesostases, cooled relatively rapidly from melt temperatures and were not significantly reheated. Other chondrules, including some irregular chondrules and at least one droplet chondrule, were thermally metamorphosed prior to the final agglomeration of Chainpur. Two of the most annealed chondrules contain relatively abundant Na-feldspar, and one of these chondrules contains phenocrysts of equilibrated olivine with a composition appropriate to that of an LL4 chondrite. Static annealing of chondrules may have taken place immediately following chondrule formation during moderately slow cooling (~100 °C/hr) or in reheating episodes.

Acknowledgements—This work was supported in part by NSF grant EAR 7421801 A01 to R. T. Dodd and NASA grant NAG9-37 to W. V. Boynton. The writer wishes to thank Melinda Hutson, Bob Dodd, Bill Boynton, David Kring, Tim Swindle, Alan Rubin, Jeff Grossman, Roger Hewins and most recently Hap McSween and Rhian Jones for constructive criticisms of various iterations of this manuscript. Special thanks are also given to John Lewis and Bill Boynton for providing the writer with encouragement and access to computers after he moved to Arizona.

Editorial handling: K. Keil.

REFERENCES

Ashworth J. R. (1980) Chondrite thermal histories: Clues from electron microscopy of orthopyroxene. *Earth Planet. Sci. Lett.* **46,** 167–177.

Ashworth J. R. (1981) Fine structure in H-group chondrites. *Proc. R. Soc. Lond. A* **374,** 179–194.

Ashworth J. R. (1985) Transmission electron microscopy of L-group chondrites, 1. Natural shock effects. *Earth Planet. Sci. Lett.* **73,** 17–52.

Ashworth J. R. and Barber D. J. (1975) Electron petrography of shock-deformed olivine in stony meteorites. *Earth Planet. Sci. Lett.* **27,** 43–50.

Ashworth J. R. and Barber D. J. (1976) Lithification of gas-rich meteorites. *Earth Planet. Sci. Lett.* **30,** 222–233.

Ashworth J. R. and Barber D. J. (1977) Electron microscopy of some stony meteorites. *Phil. Trans. R. Soc. Lond. A* **286,** 493–506.

Ashworth J. R. and Mallinson L. G. (1985) Transmission electron microscopy of L-group chondrites, 2. Experimentally annealed Kyushu. *Earth Planet. Sci. Lett.* **73,** 33–40.

Ashworth J. R., Mallinson L. G., Hutchinson R. and Biggar G. M. (1984) Chondrite thermal histories constrained by experimental annealing of Quenggouk orthopyroxene. *Nature* **308,** 259–261.

Barber D. J. (1981) Matrix phyllosilicates and associated minerals in C2M carbonaceous chondrites. *Geochim. Cosmochim. Acta* **45,** 945–970.

Bauer J. F. (1979) Experimental shock metamorphism of mono- and polycrystalline olivine: A comparative study. *Proc. Lunar Planet. Sci. Conf.* **10th,** 2573–2596.

Biggar G. (1986) Chemistry of protopyroxene, orthopyroxene, and pigeonite, crystallized from liquids close to chondrule compositions. *Bull. Mineral.* **109,** 529–541.

Binns R. A. (1967) Structure and evolution of non-carbonaceous chondritic meteorites. *Earth Planet. Sci. Lett.* **2,** 23–28.

Binns R. A. (1970) Pyroxenes from non-carbonaceous chondritic meteorites. *Mineral. Mag.* **37,** 649–669.

Boland J. N. and Duba A. (1981) Solid-state reduction of iron in olivine—planetary and meteoritic evolution. *Nature* **294,** 142–144.

Bunch T. E. and Rajan R. J. (1988) Meteorite regolithic breccias. In *Meteorites and the Early Solar System* (eds. J. F. Kerridge and M. S. Matthews), pp. 144–164. University of Arizona Press, Tucson.

Buseck P. R., Nord G. L., Jr. and Veblen D. R. (1980) Subsolidus phenomena in pyroxenes. In *Reviews of Mineralogy* 7 (ed. C. T. Prewitt). Mineralogical Society of America, Washington, D.C.

Cameron M. and Papike J. J. (1980) Crystal chemistry of silicate pyroxenes. In *Reviews of Mineralogy* 7 (ed. C. T. Prewitt). Mineralogical Society of America, Washington, D.C.

Carter N. L., Raleigh C. B. and De Carli P. S. (1968) Deformation of olivine in stony meteorites. *J. Geophys. Res.* **73,** 5439–5461.

Carter N. L., Lueng I. S. and Lallemant Ave (1970) Deformation of silicates from the Sea of Tranquility. *Science* **167,** 666–668.

Champness P. E. and Lorimer G. W. (1976) Exsolution in silicates. In *Electron Microscopy in Mineralogy* (ed. H.-R. Wenk), pp. 174–204. Springer-Verlag, Berlin.

Chao E. C. T., James O. B., Minken J. A., Boreman J. A., Jackson E. D. and Raleigh C. B. (1970) Petrology of unshocked crystalline rocks and evidence for impact metamorphism in Apollo 11 returned lunar sample. *Proc. Apollo 11 Lunar Sci. Conf.,* 287–314.

Christie J. M. and Ardell A. J. (1976) Deformation structures in minerals. In *Electron Microscopy in Mineralogy* (ed. H.-R. Wenk), pp. 374–404. Springer-Verlag, Berlin.

Christophe Michel-Lévy M. (1981) Some clues to the history of H-group chondrites. *Earth Planet. Sci. Lett.* **54,** 67–80.

Cintala M. J., Head J. W. and Wilson L. (1979) The nature and effects of impact cratering on small bodies. In *Asteroids* (ed. T. Gehrels), pp. 579–600. University of Arizona Press, Tucson.

Coe R. H. and Kirby S. H. (1975) The orthoenstatite to clinoenstatite transformation by shearing and reversion by annealing: Mechanism and potential applications. *Contrib. Mineral. Petrol.* **52,** 29–55.

Dodd R. T. (1971) The petrology of chondrules in the Sharps meteorite. *Contrib. Mineral. Petrol.* **31,** 201–227.

Dodd R. T. (1972) Calcium in chondritic olivine. *Geol. Soc. Amer. Memoir* **132,** 651–660.

Dodd R. T. (1973) Minor element abundances in olivines of the Sharps (H-3) chondrite. *Contrib. Mineral. Petrol.* **42,** 159–167.
Dodd R. T. (1974) The petrology of chondrules in the Hallingeberg meteorite. *Contrib. Mineral. Petrol.* **47,** 97–112.
Dodd R. T. (1978a) The composition and origin of large microporphyritic chondrules in the Manych (L3) chondrite. *Earth Planet. Sci. Lett.* **39,** 52–66.
Dodd R. T. (1978b) Compositions of droplet chondrules in the Manych (L3) chondrite and the origin of chondrules. *Earth Planet. Sci. Lett.* **40,** 71–82.
Dodd R. T. (1981) *Meteorites. A Petrologic-Chemical Synthesis.* Cambridge University Press, Cambridge.
Dodd R. T. (1982) The compositions of incipient shock melts in L6 chondrites. *Earth Planet. Sci. Lett.* **59,** 355–363.
Dodd R. T. and Jarosewich E. (1979) Incipient melting in and shock classification of L-group chondrites. *Earth Planet. Sci. Lett.* **44,** 335–340.
Goetze C. and Kohlstedt D. L. (1973) Laboratory study of dislocation climb and diffusion in olivine. *J. Geophys. Res.* **78,** 5961–5971.
Heuer A. H., Christie J. M., Lally J. S. and Nord G. L., Jr. (1974) Electron petrographic study of some Apollo 17 breccias. *Proc. Lunar Sci. Conf.* **5th,** 275–286.
Hewins R. H. (1988) Experimental studies of chondrules. In *Meteorites and the Early Solar System* (eds. J. F. Kerridge and M. S. Matthews), pp. 660–679. University of Arizona Press, Tucson.
Heymann D. (1967) On the origin of Hypersthene chondrites: Ages and shock effects of black chondrites. *Icarus* **6,** 189–221.
Heymann D. and Mazor E. (1968) Noble gases in unequilibrated ordinary chondrites. *Geochim. Cosmochim. Acta* **32,** 1–19.
Heyse J. V. (1979) The metamorphic history of the LL-group ordinary chondrites. Ph.D. thesis, State University of New York at Stony Brook.
Hörz F. and Schaal R. B. (1981) Asteroidal agglutinate formation and implications for asteroidal surfaces. *Icarus* **46,** 337–353.
Huebner J. S. (1980) Pyroxene phase equilibria at low pressure. In *Reviews of Mineralogy,* **7** (ed. C. T. Prewitt). Mineralogical Society of America, Washington, D.C.
Hull D. (1975) *Introduction to Dislocations.* Oxford: Pergamon Press.
Hutchinson R. and Bevan A. W. R. (1983) Conditions and time of chondrule accretion. In *Chondrules and Their Origins* (ed. E. A. King), pp. 162–179. Lunar and Planetary Institute, Houston.
Jobbins E. A., Dimes F. G., Binns R. A., Hey M. H. and Reed S. J. B. (1966) The Barwell meteorite. *Mineral. Mag.* **35,** 881–902.
Kerridge J. A. and Kieffer S. W. (1977) A constraint on impact theories of chondrule formation. *Earth Planet. Sci. Lett.* **35,** 35–42.
Kitamura M., Yasuda M., Watanabe S. and Morimoto N. (1983) Cooling history of pyroxene chondrules in the Yamato-74191 chondrite (L3)—An electron microscopic study. *Earth Planet. Sci. Lett.* **63,** 189–201.
Kracher A., Scott E. R. D. and Keil K. (1984) Relict and other anomalous grains in chondrules: Implications for chondrule formation. *Proc. Lunar Planet. Sci. Conf.* **14th,** 559–566.
Lally J. S., Christie J. M., Nord G. L. Jr. and Heuer A. H. (1976) Deformation, recovery and recrystallization of lunar dunite 72417. *Proc. Lunar Sci. Conf.* **7th,** 1845–1863.
Levi F. A. (1973) Thermal fatigue: A possible source of structural modification in meteorites. *Meteoritics* **8,** 209–221.
Lofgren G. (1985) Dynamic crystallization experiments on chondrule melts: The effects of kinetic growth factors on the chemistry of olivine and pyroxene. *Meteoritics* **20,** 699–700.
McSween H. Y., Jr., Sears D. W. G. and Dodd R. T. (1988) Thermal metamorphism. In *Meteorites and the Early Solar System* (eds. J. F. Kerridge and M. S. Matthews), pp. 102–113. University of Arizona Press, Tucson.
Müller W. F. and Hornemann U. (1969) Shock-induced planar deformation structures in experimentally shock-loaded olivines and in olivines from chondritic meteorites. *Earth Planet. Sci. Lett.* **7,** 251–264.
Nagahara H. (1981) Evidence for secondary origin of chondrules. *Nature* **292,** 135–136.
Nagahara H. (1983) Chondrules formed through incomplete melting of pre-existing mineral clusters and the origin of chondrules. In *Chondrules and Their Origins* (ed. E. A. King), pp. 211–222. Lunar and Planetary Institute, Houston.
Phakey P., Dollinger G. and Christie J. (1972) Transmission electron microscopy of experimentally deformed olivine single crystals. In *Flow and Fracture of Rocks* (eds. H. C. Heard, I. Y. Borg, N. L. Carter and C. B. Raleigh), pp. 117–138, University of California, Los Angeles.
Ragan D. M. (1969) Olivine recrystallization textures. *Mineral. Mag.* **37,** 238–240.
Rambaldi E. R. (1981) Relict grains in chondrites. *Nature* **293,** 558–561.
Rambaldi E. R. and Wasson J. T. (1982) Fine, nickel-poor Fe-Ni grains in the olivine of unequilibrated ordinary chondrites. *Geochim. Cosmochim. Acta* **46,** 929–939.
Reimold W. U. and Stöffler D. (1978) Experimental shock metamorphism of dunite. *Proc. Lunar Planet. Sci. Conf.* **9th,** 2805–2824.
Ruzicka A. (1988) Pre-agglomeration metasomatism of chondrules in the Chainpur (LL3.4) chondrite. M.S. thesis, State University of New York at Stony Brook.
Schaal R. B. and Hörz F. (1977) Shock metamorphism of lunar and terrestial basalts. *Proc. Lunar Planet. Sci. Conf.* **8th,** 1697–1729.
Schaal R. B., Hörz F., Thompson T. D. and Bauer J. F. (1979) Shock metamorphism of granulated lunar basalt. *Proc. Lunar Planet. Sci. Conf.* **10th,** 2547–2571.
Sclar C. B. (1970) Shock metamorphism of lunar rocks and fines from Tranquility Base. *Proc. Apollo 11 Lunar Sci. Conf.,* 849–864.
Scott E. R. D. (1984) Classification, metamorphism, and brecciation of type 3 chondrites from Antarctica. *Smithsonian Contrib. Earth Sci.* **26,** 73–94.
Sears D. W., Grossman J. N., Melcher C. L., Ross L. M. and Mills A. A. (1980) Measuring metamorphic history of unequilibrated ordinary chondrites. *Nature* **287,** 791–795.
Sears D. W., Ashworth J. R., Broadbent C. P. and Bevan A. W. R. (1984) Studies of artificially shock-loaded H group chondrite. *Geochim. Cosmochim. Acta* **48,** 343–360.
Smyth J. R. (1974) Experimental study of the polymorphism of enstatite. *Amer. Mineral.* **59,** 345–352.
Steele I. M. and Smith J. V. (1975) Minor elements in lunar olivine as a petrologic indicator. *Proc. Lunar Sci. Conf.* **6th,** 451–467.
Stöffler D., Bischoff A., Buchwald V. and Rubin A. E. (1988) Shock effects in meteorites. In *Meteorites and the Early Solar System* (eds. J. F. Kerridge and M. S. Matthews), pp. 165–202. University of Arizona Press, Tucson.
Swindle T. D., Caffee M. W., Hohenberg C. M., Lindstrom M. M. and Taylor G. J. (1989) Iodine-xenon studies of petrographically and chemically characterized Chainpur chondrules. *Geochim. Cosmochim. Acta,* submitted.
Töpel-Schadt J. and Müller W. F. (1985) The submicroscopic structure of the unequilibrated ordinary chondrites Chainpur, Mezo-Madaras and Tieschitz: A transmission electron-microscopic study. *Earth Planet. Sci. Lett.* **74,** 1–12.
Watanabe S., Kitamura M. and Morimoto N. (1984) Analytical electron microscopy of a chondrule with relict olivine in the ALH-77015 chondrite (L3). *Proc. Symp. Antarctic Meteorites* **9th,** 200–208.
Wlotzka F. (1983) Composition of chondrules, fragments and matrix in the unequilibrated ordinary chondrites Tieschitz and Sharps. In *Chondrules and Their Origins* (ed. E. A. King), pp. 296–318. Lunar and Planetary Institute, Houston.
Yasuda M., Kitamura M. and Morimoto N. (1983) Electron microscopy of clinoenstatite from a boninite and a chondrite. *Phys. Chem. Minerals* **9,** 192–196.